

Journal of Materials Chemistry A

Accepted Manuscript



This is an *Accepted Manuscript*, which has been through the Royal Society of Chemistry peer review process and has been accepted for publication.

Accepted Manuscripts are published online shortly after acceptance, before technical editing, formatting and proof reading. Using this free service, authors can make their results available to the community, in citable form, before we publish the edited article. We will replace this *Accepted Manuscript* with the edited and formatted *Advance Article* as soon as it is available.

You can find more information about *Accepted Manuscripts* in the [Information for Authors](#).

Please note that technical editing may introduce minor changes to the text and/or graphics, which may alter content. The journal's standard [Terms & Conditions](#) and the [Ethical guidelines](#) still apply. In no event shall the Royal Society of Chemistry be held responsible for any errors or omissions in this *Accepted Manuscript* or any consequences arising from the use of any information it contains.

Cite this: DOI: 10.1039/c0xx00000x

ARTICLE TYPE

www.rsc.org/xxxxxx

Cyclic performance of $\text{CaCO}_3@ \text{mSiO}_2$ for CO_2 capture in calcium looping cycle

Chien-Cheng Li^a, Ui-Ting Wu^b and Hong-Ping Lin^{*b}

Received (in XXX, XXX) Xth XXXXXXXXX 20XX, Accepted Xth XXXXXXXXX 20XX

DOI: 10.1039/b000000x

A simple and cost-effective one-pot synthesis route to directly prepare $\text{CaCO}_3@ \text{mesoporous silica}$ in a core/shell structure (denoted as $\text{CaCO}_3@ \text{mSiO}_2$) as a high-performance CO_2 sorbent has been developed. The ($\text{CaCO}_3@ \text{mSiO}_2$)-based sorbents with and without pelletization showed superior CO_2 adsorption performance compared to a CaCO_3 -based sorbent. The carbonation conversion of the ($\text{CaCO}_3@ \text{mSiO}_2$)-based sorbents have been significantly improved by coating the mesoporous silica onto the CaCO_3 -based sorbents, as well as the retention of the carbonation conversion. The best adsorption performance is obtained by using the ($\text{CaCO}_3@ 5.6 \text{ wt\% mSiO}_2$)-based sorbent. The improved carbonation conversion retention of ($\text{CaCO}_3@ 5.6 \text{ wt\% mSiO}_2$)-based pellet sorbent is around 25% after 50 cycles of decarbonation/carbonation higher than that of the CaCO_3 -based sorbent (13%). The resultant ($\text{CaCO}_3@ \text{mSiO}_2$)-based sorbent has high resistance toward carbonation/decarbonation reaction.

1 Introduction

Atmospheric concentrations of carbon dioxide caused by the combustion of fossil fuels, such as oil, coal and gas, have increased by around 21% from approximately 317 ppm in 1959 to an atmospheric average of approximately 385 ppm in 2009^{1, 2}. Flue gas from fossil fuel combustion power plants represents a major source of CO_2 emissions²⁻⁴.

Among many different CO_2 capture processes, the calcium looping process (CLP) is one that is techno-economically feasible for industrial applications and has good commercialization potential. Capture of CO_2 over CaO-based sorbent has attracted enormous interest in the development of removing CO_2 from flue gas and energy pumps, such as pre-combustion CO_2 capture, post-combustion CO_2 capture, and energy storage for application of the CLP^{3, 5-9}. Despite high activity, adsorption capacity, CO_2 capture efficiencies, and low cost of the CaO-based sorbents for CO_2 capture, their shortcomings are poor long-term stability and rapid loss-in-capacity limiting the widespread application of the CLP. Rapid decay in reactivity over several carbonation/decarbonation cycles has been observed due to severe sintering^{2, 3, 5-20}.

Several studies have been conducted to enhance the resistance of CaO to sintering, such as modification of the structure and incorporation of inert materials, which are Al_2O_3 , MgO, ZrO_2 , TiO_2 , SiO_2 , CeO_2 , CrO_2 , CuO, CoO, Mn_2O_3 , CaTiO_3 , BaO, La_2O_3 , K_2CO_3 , and Fe_2O_3 ^{2, 3, 8, 9, 16-19, 21-29}. The performance of the modified CaO-based sorbents is highly dependent on different synthetic methods as well as the precursors^{2, 3, 8, 13, 22}. In addition, dispersion and incorporation of CaO in the inert solid matrix (or

inert solid material in CaO matrix) and the total CaO surface area have been shown to be critical to the activity and durability of the sorbent. Therefore, the development of sorbents with effective dispersion, incorporation, and optimized surface area for improving the durability and activity of sorbents is highly desirable.

Mesoporous materials provide high surface areas, large pore volumes and tuneable pore sizes for potential applications in absorbents, catalysts, chemical sensors, drug-delivery systems, and various electrochemical devices. By a proper tuning of the fabrication conditions, such as proper reaction conditions and organic templates, it can be prepared to consist of mesoporous materials with high-flexibility in dimension, composition and morphology. Mass production of mesoporous materials has become possible by using a cheap template and inorganic sources and operating under nature-friendly reaction conditions. Several mesoporous materials/ CaCO_3 composite sorbents have been reported^{9, 23}.

In the present study, mesoporous silica was selected as the inert materials, which provided a highly stable framework under severe temperature conditions, as well as not markedly absorbing CO_2 under the decarbonation/carbonation conditions. We propose a simple and cost-effective one-pot synthesis route to directly coat mesoporous silica on the CaCO_3 particles by using gelatin as the surface activation agent³⁰ to form highly stable $\text{CaCO}_3@ \text{mesoporous silica}$ (denoted as $\text{CaCO}_3@ \text{mSiO}_2$) core/shell composite sorbents.

2 Experiments

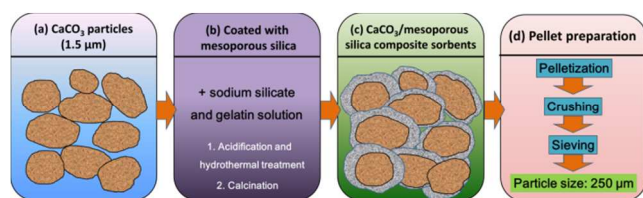


Figure 1. A schematic showing the preparation of the $(\text{CaCO}_3@m\text{SiO}_2)$ -based composite sorbents for CO_2 adsorption.

2.1 Sorbent preparation

The cyclic carbonation/decarbonation conversions of the CaCO_3 -based sorbents from a commercial limestone in Taiwan coated with mesoporous silica were investigated in order to enhance its durability for CO_2 capture. The weight percentages of the chemical compositions in the limestone are shown in Table 1. The limestone was ground and sieved to the average particle size of around $1.5 \mu\text{m}$, which has higher adsorption performance of CO_2 capture compared with particle sizes larger than $90 \mu\text{m}$. To prepare $\text{CaCO}_3@m\text{SiO}_2$, 12.0 g of CaCO_3 was dispersed to 75.0 g of water and the pH value of the solution was adjusted to around 8.0 . Then, the CaCO_3 gel solution was combined with a gelatin aqueous solution containing 0.72 g type A gelatin and 45.0 g of water. After stirring for $6\text{--}12 \text{ h}$, the gelatin- CaCO_3 solution was added to an acidified sodium silicate solution (2.88 g of sodium silicate and 180.0 g of water) at $\text{pH} \approx 8.0$ and further stirred for 1 h . The gel solution was hydrothermally treated at 100°C for 1 day . Filtration, calcination at 600°C gave the $\text{CaCO}_3@m\text{SiO}_2$ sorbent.

Table 1 Composition of the CaCO_3 -based sorbent (limestone) (wt%).

CaO (%)	MgO (%)	SiO ₂ (%)	Fe ₂ O ₃ (%)	Al ₂ O ₃ (%)	P ₂ O ₅ (%)	MnO (%)	K ₂ O (%)	Na ₂ O (%)	LOI (%)	Sum (%)
54.86	1.61	0.49	0.1	0.06	0.04	0.02	0.02	0.01	42.7	99.91

2.2 Pellet preparation

Sorbents with particle sizes of less than $90 \mu\text{m}$ may not be suitable for fluidized-bed combustion (FBC) systems in practical applications of calcium looping. A pelletization is therefore needed to prepare the CaCO_3 -based and $(\text{CaCO}_3@m\text{SiO}_2)$ -based sorbents for further cyclic decarbonation/carbonation tests and practical purposes. The CaCO_3 -based and $(\text{CaCO}_3@m\text{SiO}_2)$ -based sorbents with a particle size of $1.5 \mu\text{m}$ were pelleted without adding any binder, crushed, and sieved to the average particle size of $250 \mu\text{m}$. The sorbents were first compressed into pellets with a diameter of 12 mm . Pellet strength was tested by examining the effect of the fall of a pellet from a height of 1 m to a concrete surface¹¹. The tests show that the pelletized $(\text{CaCO}_3@m\text{SiO}_2)$ -based sorbents exhibited higher pellet strength than did the CaCO_3 -based sorbents resulting from high crushing strength. It is suggested that mesoporous silica can serve as a good mineral additive for pelletization of the $(\text{CaCO}_3@m\text{SiO}_2)$ -based sorbents. The CaCO_3 -based and $(\text{CaCO}_3@5.6 \text{ wt}\% \text{ mSiO}_2)$ -based sorbents were pelleted for further cyclic decarbonation/carbonation testing.

2.3 Characterization of sorbents

The cyclic carbonation/decarbonation tests were carried out in a SERARAM SETSYS Evolution thermogravimetric analyzer (TGA). The sample holder is a platinum basket of 8 mm in diameter and 3 mm in height. For each run in the TGA, around 30 mg of sorbent was introduced into the sample holder. The gases (CO_2 , N_2) were controlled by a mass flow meter and fed to the top of the alumina tube. The gas flow rate of CO_2 and N_2 was 100 mL/min . Each cycle included decarbonation under N_2 followed by carbonation for CO_2 capture. For the first decarbonation, temperature was increased from ambient to the chosen temperature (850°C) at the heating rate of about 10°C/min under a N_2 flow equal to 100 mL/min . Then, temperature was maintained for 35 min at 850°C . After cooling to carbonation temperature (650°C), the gas flow was switched to CO_2 with 100 mL/min . The decarbonated sample was then exposed to the reactant gas (CO_2) for 40 min for carbonation. The cyclic decarbonation/carbonation tests were performed in a TGA for about 50 cycles in the experiments. Temperature and sample weight were continuously recorded in a computer. The carbonation conversion (%) was calculated using the following equation^{21, 27}:

$$\text{Carbonation conversion (\%)} = \frac{m_n - m_0}{m_0 \cdot b} \cdot \frac{W_{\text{CaO}}}{W_{\text{CO}_2}} \times 100 \quad (1)$$

where m_n is the mass of the carbonated sorbent after n cycles, m_0 is the mass of the calcined initial sorbent, and b is the content of CaO in the initial calcined sorbent. W_{CaO} and W_{CO_2} are the mole masses of CaO and CO_2 , respectively.

2.4 Apparatus

The sorbents were examined using a JOEL 6500 field-emission scanning electron microscope (FE-SEM) equipped with X-ray energy dispersive microanalysis (EDAX). The morphology and mesostructure of the prepared novel $\text{CaCO}_3@m\text{SiO}_2$ sorbents were observed using a transmission electron microscope (TEM, Hitachi H-7500) operated at an accelerating voltage of 80 kV . X-ray diffraction (XRD) patterns were obtained using a Bruker D2 phaser diffractometer with $\text{Cu } \alpha$ radiation ($\lambda = 0.1542 \text{ nm}$) operated at 30 kV and 10 mA . Chemical compositions of the limestone (CaCO_3 -based sorbent) were determined by X-ray fluorescence (XRF) elemental analyses. X-ray photoelectron spectra (XPS) were obtained by a ULVAC-PHI PHI-Quantera SXM XPS system equipped the monochromatized $\text{Al } K\alpha$ radiation (1486.6 eV). All binding energy (BE) values were calibrated using the $\text{C } 1s$ peak at 284.6 eV as a reference.

3 Results and discussion

The $(\text{CaCO}_3@m\text{SiO}_2)$ -based composite sorbents were fabricated using a one-pot synthetic route. The proposed scheme of synthesis of the well-encapsulated $\text{CaCO}_3@m\text{SiO}_2$ core/shell structure and the preparation procedures of the CO_2 sorbent are illustrated in Fig. 1. The efficient well-encapsulated $\text{CaCO}_3@m\text{SiO}_2$ core/shell composites are supposed to exhibit high accessibility between gases (CO_2 or N_2) and sorbents. Figure 2(a) demonstrates TEM images of the $\text{CaCO}_3@m\text{SiO}_2$ sample at silica/ CaCO_3 weight ratio of 5.6% . At higher magnification, it is clearly seen that the CaCO_3 nanoparticles are well coated by

mesoporous silica shell (Fig. 2(b)). After HCl-etching, the remaining mesoporous silica shell replicates the form of the original CaCO_3 nanoparticles and the thickness of the silica shell is around tens nanometres (Fig. 2c). From N_2 adsorption-desorption isotherm of the mesoporous silica shell, a capillary condensation occurring at $P/P_0 = 0.7$ is ascribed to pore size of around 8.0 nm (Fig. 2(d)). The BET surface area and pore size distribution of the mesoporous silica shell is similar to that of the gelatin-templated mesoporous silica that indicates gelatin is capable to activate the CaCO_3 particle surface for silica deposition. From the TEM observation results, we found the thickness and casting integrity of the mesoporous silica shell are dependent on the silica/ CaCO_3 weight ratio.

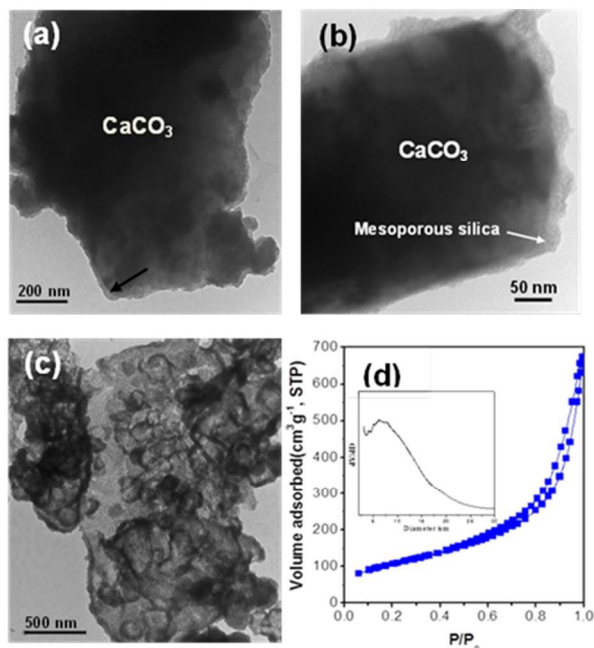


Fig. 2 TEM images of the $\text{CaCO}_3@m\text{SiO}_2$ before (a), (b) and after (c) HCl-etching. (d) N_2 adsorption-desorption isotherm of the $\text{CaCO}_3@m\text{SiO}_2$ after HCl-etching. Arrows in Fig. 2(a) and (b) indicates the mesoporous silica shell. The inset in Fig. 2(d) is the BJH pore size distribution of the mesoporous silica shell.

To further prove the distribution homogeneity of the silica in the prepared samples, a representative SEM and EDX mapping images of the $\text{CaCO}_3@5.6 \text{ wt\% mSiO}_2$ -based sorbent were demonstrated in Fig. 3. Fig. 3(a) shows the dispersed particles of about 0.5–2.5 μm . To demonstrate the even distribution of Ca and Si elements, an SEM image (Fig. 3(a)) and its digital color EDAX mapping images of calcium, silicon, magnesium, oxygen, and carbon for the $(\text{CaCO}_3@5.6 \text{ wt\% mSiO}_2)$ -based sorbent are shown in Fig. 3(b)–(f), respectively. Similar element distribution images indicate that calcium and silicon elements were well dispersed in the supported calcium carbonate matrix. The EDAX analysis of the $(\text{CaCO}_3@5.6 \text{ wt\% mSiO}_2)$ -based sorbent shows that the composition of the sample synthesized from the weight ratio of silica to CaCO_3 of 5.6/94.4 in CaCO_3 -silica-gelatin precursor is 4.5/95.5. The sorbent composition is close to that of the original precursor. For convenience, the sorbent composition is expressed by the weight ratio of silica to CaCO_3 in CaCO_3 -

silicate-gelatin precursor.

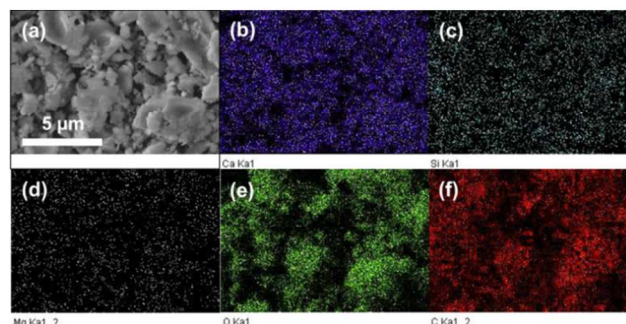


Fig. 3 SEM image (a) and its digital color EDX mapping images of calcium, silicon, magnesium, oxygen and carbon (b–f) of the $(\text{CaCO}_3@5.6 \text{ wt\% mSiO}_2)$ -based sorbent.

To get optimum $\text{CaCO}_3/\text{silica}$ compositions in the $(\text{CaCO}_3@m\text{SiO}_2)$ -based sorbents, the samples at different weight ratios of silica/ CaCO_3 of 0, 4.7, 5.6, 7.2, and 10.5 wt% were examined. Fig. 4 shows the cyclic evolution of the carbonation conversion of $(\text{CaCO}_3@m\text{SiO}_2)$ -based sorbents coated with mesoporous silica at various weight ratios of silica to CaCO_3 for the decarbonation/carbonation tests. The carbonation conversion of the $(\text{CaCO}_3@m\text{SiO}_2)$ -based sorbents has been improved by the incorporation of the mesoporous silica onto the CaCO_3 -based sorbents after the tenth decarbonation/carbonation cycle, as well as the ratio of the decay of the carbonation conversion. The carbonation conversion of the CaCO_3 -based sorbents (i.e. no silica coating) decayed rapidly from 92% to 24% for the decarbonation/carbonation test after 50 cycles. The best adsorption performance was obtained using the $(\text{CaCO}_3@5.6 \text{ wt\% mSiO}_2)$ -based sorbent. The ratio of its carbonation conversion remained 37% for the decarbonation/carbonation test after 50 cycles. The sorbents prepared from the $\text{CaCO}_3@m\text{SiO}_2$ at a $\text{SiO}_2/\text{CaCO}_3$ ratio higher than 5.6 wt% inhibited further improvement in the adsorption performance, which had less active CaO in the sorbents. Some studies have shown that pelletization with a bentonite binder resulted in poor carbonation conversion due to high SiO_2 content in the pellet limestones. It is suggested that high SiO_2 content may reduce accessibility between gases (CO_2 or N_2) and sorbents (i.e. less accessible CaO in the sorbents), and decrease the melting point of the Ca-Si compounds to induce the formation of CaO/SiO_2 eutectic mixtures^{10, 12}. While at the $\text{SiO}_2/\text{CaCO}_3$ ratio lower than 5.6 wt%, the sorbent exhibit a lower improvement in the adsorption performance because the CaCO_3 particles were not well-encapsulated by the mesoporous silica.

For practical applications of calcium looping, sorbents with particle sizes of less than 90 μm may not be suitable for FBC systems. Therefore, the $(\text{CaCO}_3@m\text{SiO}_2)$ -based sorbents with particle size of 1.5 μm were used for pelletization into a larger particle size of 250 μm for further cyclic carbonation/decarbonation testing. Fig. 5 shows the cyclic evolution of the carbonation conversion of the CaCO_3 -based sorbents and the $(\text{CaCO}_3@5.6 \text{ wt\% mSiO}_2)$ -based sorbents with and without pelletization toward the decarbonation/carbonation test after 50 cycles. For the CaCO_3 -based sorbents, the carbonation conversion efficiency of the CaCO_3 -based sorbent

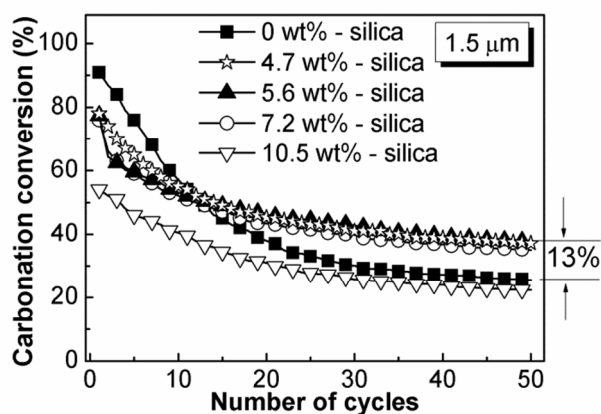


Fig. 4 The cyclic evolution of the carbonation conversion of the $(\text{CaCO}_3@m\text{SiO}_2)$ -based sorbents (original particle size: $1.5 \mu\text{m}$) coated with mesoporous silica at various weight ratios of silica to CaCO_3 on decarbonation/carbonation test after 50 cycles.

(original particle size: $250 \mu\text{m}$) and CaCO_3 -based pellet sorbent ($250 \mu\text{m}$) rapidly decayed from 68% to 12% and from 93% to 10%, respectively, after 50 cycles of decarbonation/carbonation. The $(\text{CaCO}_3@5.6 \text{ wt}\% \text{ mSiO}_2)$ -based sorbents with and without pelletization provided a noticeably higher carbonation conversion than that of the CaCO_3 -based sorbents after 50 cycles of decarbonation/carbonation except for the first two cycles. The retention of the carbonation conversion was improved by the incorporation of the mesoporous silica on the CaCO_3 -based sorbents. The $(\text{CaCO}_3@5.6 \text{ wt}\% \text{ mSiO}_2)$ -based sorbents with and without pelletization had a close carbonation conversion efficiency to that of the CaCO_3 -based sorbents, and decayed slightly less, from around 80% to 37% after 50 cycles of decarbonation/carbonation. This suggests that pelletization may not affect the CO_2 adsorption performance for $(\text{CaCO}_3@5.6 \text{ wt}\% \text{ mSiO}_2)$ -based sorbents. The improvement in the carbonation conversion rate of the $(\text{CaCO}_3@5.6 \text{ wt}\% \text{ mesoporous silica})$ -

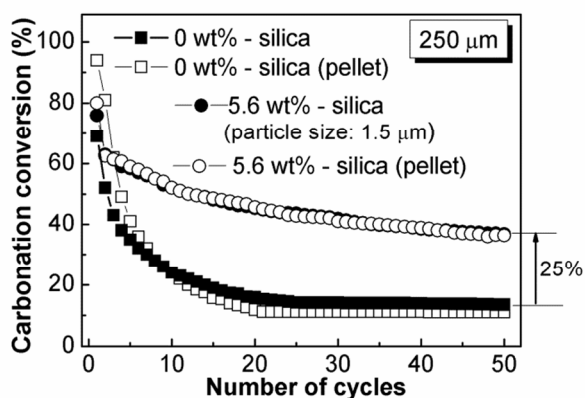


Fig. 5 The cyclic evolution of the carbonation conversion of the CaCO_3 -based sorbent (\blacksquare) (original particle size: $250 \mu\text{m}$), the CaCO_3 -based pellet sorbent (\square) (original particle size: $1.5 \mu\text{m}$; pellet size: $250 \mu\text{m}$), the $(\text{CaCO}_3@5.6 \text{ wt}\% \text{ mSiO}_2)$ -based sorbent (\bullet) (original particle size: $1.5 \mu\text{m}$), and the $(\text{CaCO}_3@5.6 \text{ wt}\% \text{ mSiO}_2)$ -based pellet sorbent (\circ) (original particle size: $1.5 \mu\text{m}$; pellet size: $250 \mu\text{m}$) on decarbonation/carbonation reaction after

50 cycles.

based pellet sorbent was around 25% after 50 cycles of decarbonation/carbonation testing compared with the CaCO_3 -based sorbent. This was probably due to a highly stable framework structure of mesoporous silica, which hinders a significant change in surface area of the CaCO_3 sorbents during decarbonation/carbonation reactions.

Fig. 6 shows the surface morphologies of the CaCO_3 -based sorbent and $(\text{CaCO}_3@5.6 \text{ wt}\% \text{ mSiO}_2)$ -based sorbent before the first and after the fiftieth decarbonation/carbonation cycle. The appearance of the surface morphology of both the CaCO_3 -based sorbent and the $(\text{CaCO}_3@5.6 \text{ wt}\% \text{ mSiO}_2)$ -based sorbent was observed after calcining at $500 \text{ }^\circ\text{C}$ for 0.5 h in air (before the first cycle), and appeared to have isolated particles. The particle sizes of both sorbents ranged from 0.5 to $2 \mu\text{m}$. Comparison of surfaces of the CaCO_3 -based sorbent and the $(\text{CaCO}_3@5.6 \text{ wt}\% \text{ mSiO}_2)$ -based sorbents after the fiftieth cycle revealed sintering of the agglomeration particles, reaction particles, and fine particles in the CaCO_3 -based sorbent. The CaCO_3 -based sorbent consisted of dispersed particles of about $1 \mu\text{m}$ or less after the fiftieth cycle. Although the isolated large particles were kept stable in the $(\text{CaCO}_3@5.6 \text{ wt}\% \text{ mSiO}_2)$ -based sorbent, the particle size became a little bit larger. For the CaCO_3 -based sorbent, there was a significant decrease of carbonation conversion with cycle number, which was considered to depend on the decrease of the surface area and porosity caused by the growth and fusion of particles. Large particles in $(\text{CaCO}_3@5.6 \text{ wt}\% \text{ mSiO}_2)$ -based sorbent seemed to cause fusion within the sample so that the sintering between mutual particles was slightly less than that of CaCO_3 -based sorbent. This suggests that the dispersed mesoporous silica in $(\text{CaCO}_3@5.6 \text{ wt}\% \text{ mSiO}_2)$ -based sorbent surrounded the particles of CaCO_3 and prevented them from mutually sintering. Therefore, mesoporous silica can be used as a stable framework structure and diffusion barrier to improve the stable reversibility of the cyclic reaction.

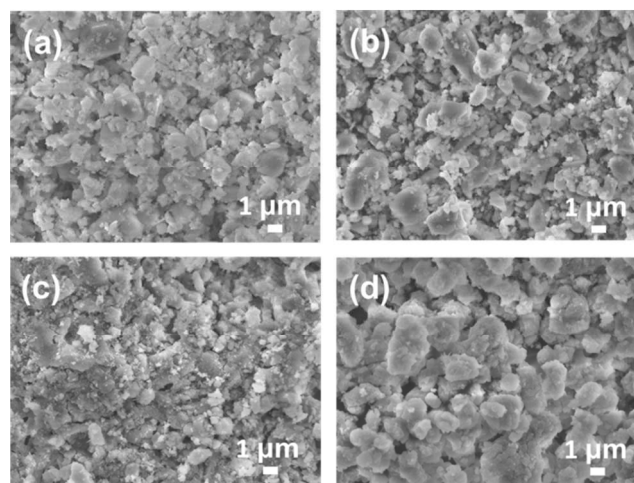


Fig. 6 SEM images of the surface of the CaCO_3 -based sorbent (a) and the $(\text{CaCO}_3@5.6 \text{ wt}\% \text{ mSiO}_2)$ -based sorbent (b) after calcining at $500 \text{ }^\circ\text{C}$ for 0.5 h in air (before the first cycle). SEM images of the surface of the CaCO_3 -based sorbent (c) and the $(\text{CaCO}_3@5.6 \text{ wt}\% \text{ mSiO}_2)$ -based sorbent (d) after calcining at $500 \text{ }^\circ\text{C}$ for 0.5 h in air and 50 decarbonation/carbonation test

cycles.

The X-ray diffraction patterns of the CaCO_3 -based sorbent and $(\text{CaCO}_3@m\text{SiO}_2)$ -based sorbents prepared from the CaCO_3 particles and silicate–gelatin precursor (Fig. 7) were observed after calcining at 500°C for 0.5 h in air. All samples showed characteristic peaks of calcium carbonate. No distinguishable diffraction peaks of the phases with the crystalline Si or Si–Ca compounds were obtained, though the $(\text{CaCO}_3@m\text{SiO}_2)$ -based sorbents had silica content in the range of 3.8 to 10.5 wt%, as shown in Fig. 7 (b)–(e). The X-ray diffraction patterns of the CaCO_3 -based sorbents and the $(\text{CaCO}_3@m\text{SiO}_2)$ -based sorbents after calcining at 500°C for 0.5 h in air and operating the cyclic decarbonation/carbonation test after the fiftieth cycle are shown in Fig. 8. It was found that the CaCO_3 and calcium silicate phases are present in the used sorbents. Despite the appreciable silica content in the sorbents, the intensity of CaCO_3 peaks is higher and sharper than that of the calcium silicate peaks. Essentially, the calcium silicate is one kind of feedstock for accelerated carbonation as well^{31, 32}. It is suggested that the phase components of the $(\text{CaCO}_3@m\text{SiO}_2)$ -based sorbents did not markedly transform after calcining at 500°C for 0.5 h in air and operating the cyclic decarbonation/carbonation test after the fiftieth cycle.

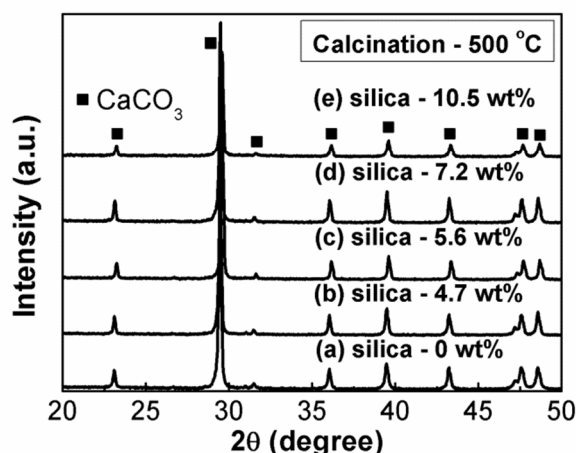


Fig. 7 The X-ray diffraction patterns of the CaCO_3 -based sorbents and the $(\text{CaCO}_3@m\text{SiO}_2)$ -based sorbents after calcining at 500°C for 0.5 h in air.

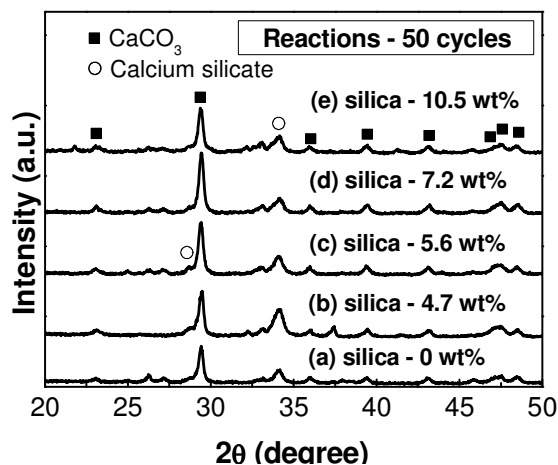


Fig. 8 The X-ray diffraction patterns of the CaCO_3 -based sorbents and the $(\text{CaCO}_3@m\text{SiO}_2)$ -based sorbents after calcining at 500°C

for 0.5 h in air and 50 decarbonation/carbonation test cycles.

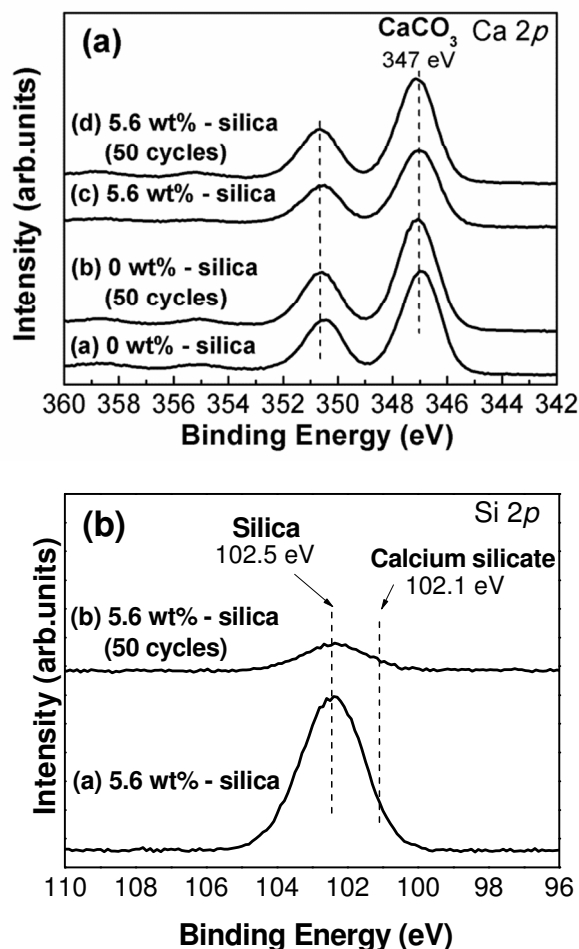


Fig. 9 XPS spectra of the Ca $2p$ (a) and Si $2p$ (b) core level obtained from the CaCO_3 -based sorbent and $(\text{CaCO}_3@5.6\text{ wt}\% \text{ mSiO}_2)$ -based sorbent before the first and after the 50 decarbonation/carbonation test cycles.

Fig. 9 shows the XPS spectra of the Ca $2p$ and Si $2p$ core level obtained from the CaCO_3 -based sorbent and the $(\text{CaCO}_3@5.6\text{ wt}\% \text{ mSiO}_2)$ -based sorbent before the first and after the fiftieth decarbonation/carbonation cycle. The Ca $2p$ spectra of both the CaCO_3 -based sorbent and the $(\text{CaCO}_3@5.6\text{ wt}\% \text{ mSiO}_2)$ -based sorbent exhibited an oxidized character at a binding energy (BE) of 447 eV ($\Delta = 3.6$)³³, a value that corresponds to calcium carbonate as shown in Fig. 9(a). These spectra had no marked change with the incorporation of the mesoporous silica in the sorbents before the first and after the fiftieth decarbonation/carbonation cycle. These features indicate the CaCO_3 -based sorbent and the $(\text{CaCO}_3@m\text{SiO}_2)$ -based sorbent were dominated by CaCO_3 compounds. However, the peak of Si $2p$ is at BE (Si $2p_{3/2}$) = 102.5 eV ³³, a value that corresponds to silica, as shown in Fig 9(b). This indicates that the $(\text{CaCO}_3@m\text{SiO}_2)$ -based sorbents were composed mainly of calcium carbonate rather than calcium silicate or CaO/SiO_2 eutectic mixtures, parallel to the results of the X-ray diffraction patterns (Fig. 7 and 8). The highly durable adsorption capability further demonstrates a well encapsulated sorbents that is coated with a stable mesoporous silica framework. This mesoporous

silica framework can effectively isolate the active CaO component as a diffusion barrier and prevent sintering of CaO grains during the cyclic carbonation/decarbonation at high temperatures. The (CaCO₃@mSiO₂)-based sorbents synthesized from our one-pot synthetic route can have a long durability during carbonation/decarbonation reaction.

Conclusions

This paper presented an efficient one-pot synthetic route for synthesizing (CaCO₃@mSiO₂)-based sorbents with good encapsulation in mesoporous silica matrix. The durability of the (CaCO₃@mSiO₂)-based sorbents was improved by addition of mesoporous silica into CaCO₃-based sorbents. The dispersed mesoporous silica into (CaCO₃@mSiO₂)-based sorbent surrounded particles of CaCO₃ and prevented them from mutually sintering. The incorporation of the mesoporous silica onto the (CaCO₃@mSiO₂)-based sorbents can increase the carbonation conversion rate by 25% in comparison with CaCO₃-based sorbents for carbonation/decarbonation after 50 cycles. This indicates that mesoporous silica can be used as a stable framework structure and diffusion barrier for the improvement of the stable reversibility of the cyclic reaction.

Notes and references

^a Department of Chemical Engineering, National Tsing Hua University, Hsinchu 300, Taiwan. Tel: +88635715131; E-mail: ccli@ms.ntu-ccms.ntu.edu.tw

^b Department of Chemistry, National Cheng Kung University, Tainan 701, Taiwan. Tel: +886 62757575 ext 65342; E-mail: hplin@mail.ncku.edu.tw

- R. F. Keeling, S.C. Piper, A.F. Bollenbacher and J.S. Walker, *Carbon Dioxide Information Analysis Center, Oak Ridge National Laboratory, U.S. Department of Energy, Oak Ridge, Tenn., U.S.A. doi: 10.3334/CDIAC/atg.035.*, 2009.
- S. Choi, J. H. Drese and C. W. Jones, *ChemSusChem*, 2009, **2**, 796-854.
- W. Liu, H. An, C. Qin, J. Yin, G. Wang, B. Feng and M. Xu, *Energy & Fuels*, 2012, **26**, 2751-2767.
- H. Yang, Z. Xu, M. Fan, R. Gupta, R. B. Slimane, A. E. Bland and I. Wright, *Journal of Environmental Sciences*, 2008, **20**, 14-27.
- J. Blamey, E. J. Anthony, J. Wang and P. S. Fennell, *Progress in Energy and Combustion Science*, 2010, **36**, 260-279.
- F. Fang, Z.-S. Li and N.-S. Cai, *Energy & Fuels*, 2008, **23**, 207-216.
- C. C. Dean, J. Blamey, N. H. Florin, M. J. Al-Jeboori and P. S. Fennell, *Chemical Engineering Research and Design*, 2011, **89**, 836-855.
- J. M. Valverde, *Journal of Materials Chemistry A*, 2013, **1**, 447-468.
- P. E. Sanchez-Jimenez, L. A. Perez-Maqueda and J. M. Valverde, *Applied Energy*, 2014, **118**, 92-99.
- V. Manovic and E. J. Anthony, *Environmental Science & Technology*, 2007, **41**, 1420-1425.
- V. Manovic and E. J. Anthony, *Environ Sci Technol*, 2009, **43**, 7117-7122.
- V. Manovic and E. J. Anthony, *Energy & Fuels*, 2009, **23**, 4797-4804.
- F.-C. Yu, N. Phalak, Z. Sun and L.-S. Fan, *Industrial & Engineering Chemistry Research*, 2011, **51**, 2133-2142.
- A. I. Lysikov, A. N. Salanov and A. G. Okunev, *Industrial & Engineering Chemistry Research*, 2007, **46**, 4633-4638.
- N. Phalak, N. Deshpande and L. S. Fan, *Energy & Fuels*, 2012, **26**, 3903-3909.
- S. F. Wu, Q. H. Li, J. N. Kim and K. B. Yi, *Industrial & Engineering Chemistry Research*, 2007, **47**, 180-184.
- H. Lu, A. Khan, S. E. Pratsinis and P. G. Smirniotis, *Energy & Fuels*, 2008, **23**, 1093-1100.
- K. O. Albrecht, K. S. Wagenbach, J. A. Satrio, B. H. Shanks and T. D. Wheelock, *Industrial & Engineering Chemistry Research*, 2008, **47**, 7841-7848.
- L. Li, D. L. King, Z. Nie and C. Howard, *Industrial & Engineering Chemistry Research*, 2009, **48**, 10604-10613.
- A. Charitos, N. Rodriguez, C. Hawthorne, M. n. Alonso, M. Zieba, B. Arias, G. Kopanakis, G. n. Scheffknecht and J. C. Abanades, *Industrial & Engineering Chemistry Research*, 2011, **50**, 9685-9695.
- P. Sun, J. R. Grace, C. J. Lim and E. J. Anthony, *Chemical Engineering Science*, 2008, **63**, 47-56.
- C. Luo, Y. Zheng, N. Ding, Q. Wu, G. Bian and C. Zheng, *Industrial & Engineering Chemistry Research*, 2010, **49**, 11778-11784.
- C.-H. Huang, K.-P. Chang, C.-T. Yu, P.-C. Chiang and C.-F. Wang, *Chemical Engineering Journal*, 2010, **161**, 129-135.
- D. S. Sultan, C. R. Müller and J. S. Dennis, *Energy & Fuels*, 2010, **24**, 3687-3697.
- D. Wang, C. Sentorun-Shalaby, X. Ma and C. Song, *Energy & Fuels*, 2010, **25**, 456-458.
- I. Zamboni, C. Courson and A. Kiennemann, *Catalysis Today*, 2011, **176**, 197-201.
- Z. Yang, M. Zhao, N. H. Florin and A. T. Harris, *Industrial & Engineering Chemistry Research*, 2009, **48**, 10765-10770.
- B. González, J. Blamey, M. McBride-Wright, N. Carter, D. Dugwell, P. Fennell and J. C. Abanades, *Energy Procedia*, 2011, **4**, 402-409.
- Y. Li, C. Zhao, H. Chen, C. Liang, L. Duan and W. Zhou, *Fuel*, 2009, **88**, 697-704.
- Y. C. Lin, C. H. Hsu, H. P. Lin, C. Y. Tang and C. Y. Lin, *Chemistry Letters*, 2007, **36**, 1258-1259.
- M. Kakizawa, A. Yamasaki and Y. Yanagisawa, *Energy*, 2001, **26**, 341-354.
- K. B. Kale, R. Y. Raskar, V. H. Rane and A. G. Gaikwad, *Adsorption Science & Technology*, 2012, **30**, 817-830.
- J. F. Moulder, W. F. Stickle, P. E. Sobol and K. D. Bomben, *Handbook of X-ray Photoelectron Spectroscopy*, Perkin-Elmer Corporation Physical Electronics Division, U.S.A, 1992.